Measurement of the fusion probability P_{CN} for the reaction of ^{50}Ti with ^{208}Pb

R. S. Naik, W. Loveland, P. H. Sprunger, and A. M. Vinodkumar
Department of Chemistry, Oregon State University, Corvallis, Oregon 97331, USA

D. Peterson, C. L. Jiang, S. Zhu, X. Tang, and E. F. Moore
Physics Division, Argonne National Laboratory, Argonne, Illinois 60439, USA

P. Chowdhury
Department of Physics, University of Massachusetts Lowell, Lowell, Massachusetts 01854, USA
(Received 15 September 2007; published 20 November 2007)

The capture cross sections and fission fragment angular distributions were measured for the reaction of ^{50}Ti with ^{208}Pb at center of mass projectile energies ($E_{c.m.}$) of 183.7, 186.2, 190.2, 194.2, and 202.3 MeV ($E^* = 14.2$, 16.6, 20.6, 24.7, and 32.7 MeV). From fitting the backward angle fragment angular distributions, the cross sections for quasifission and fusion-fission and P_{CN}, the probability that the colliding nuclei go from the contact configuration to inside the fission saddle point, were deduced. These quantities, along with the known values of the evaporation residue production cross sections for this reaction, were used to deduce values of the survival probabilities, W_{sur}, for this reaction as a function of excitation energy. The deduced values of P_{CN} and W_{sur} and their dependence on excitation energy differ from some current theoretical predictions of these quantities.

DOI: 10.1103/PhysRevC.76.054604 PACS number(s): 25.70.Jj, 25.85.−w, 25.60.Pj

I. INTRODUCTION

The cross section for producing a heavy evaporation residue, σ_{EVR}, in a fusion reaction can be written as

$$\sigma_{EVR} = \sum_{J=0}^{J_{max}} \sigma_{capture}(E_{c.m.}, J) P_{CN}(E_{c.m.}, J) \cdot W_{sur}, \quad (1)$$

where $\sigma_{capture}(E_{c.m.}, J)$ is the capture cross section at center of mass energy $E_{c.m.}$ and spin J. P_{CN} is the probability that the projectile-target system will evolve inside the fission saddle point to form a completely fused system rather than reseparating (quasifission). W_{sur} is the probability that the completely fused system will deexcite by neutron emission rather than fission. For a quantitative understanding of the synthesis of new heavy nuclei, one needs to understand $\sigma_{capture}$, P_{CN}, and W_{sur} for the reaction system under study.

The capture cross section is, in the language of coupled channel calculations, the "barrier crossing" cross section. It is the sum of the quasifission, fusion-fission, and fusion-evaporation residue cross sections. The latter cross section is so small for the systems studied in this work that it is neglected. Cold fusion reactions, i.e., reactions involving Pb or Bi target nuclei and heavier projectiles such as Ca-Kr, have been used to synthesize elements 107–113. The projectile energy is chosen to form a completely fused system with an excitation energy E^* of ~13 MeV, resulting in a deexcitation by emitting one neutron. In these cold fusion reactions, the capture cross sections have either been measured [1–4] or can be predicted, with reasonable accuracy by semiempirical systematics [5]. Thus from a knowledge of σ_{EVR} and $\sigma_{capture}$, one can calculate the value of the product W_{sur} P_{CN}.

Several successful attempts have been made to predict the cross sections for evaporation residue formation in cold fusion reactions [5–9]. In Fig. 1(a), we show some typical examples of predictions of the formation cross sections for elements 102–113 in cold fusion reactions. Because the values of $\sigma_{capture}$ are well-known or generally agreed upon [1–5], the values of the product $W_{sur} P_{CN}$ are the same in most of these predictions. However, as seen in Fig. 1(b), the predicted values of P_{CN} differ significantly in these predictions. [5–10].

In this paper, we describe an experimental study that attempts to directly measure P_{CN} in a cold fusion reaction and thus to help resolve these discrepancies in predicted values of P_{CN}. Specifically we measured the fission cross section and fragment angular distributions for the reaction of ^{50}Ti with ^{208}Pb at center of mass energies from 182–202 MeV ($E^* = 14$–33 MeV). From these data, we have used the method of Back [11] to deduce the quasifission and complete fusion-fission components of the fragment angular distributions. From the known evaporation residue cross sections for this reaction [12–17], we can use Eq. (1) to deduce W_{sur} for this system. The values of W_{sur} and P_{CN} are then compared with current predictions of these quantities.

II. EXPERIMENTAL METHODS

The experiment was carried out in the ATSCAT scattering chamber at the ATLAS accelerator facility at the Argonne National Laboratory. The experimental setup is shown in Fig. 2. Beams of ^{50}Ti^{+12} struck thin targets of ^{208}Pb or ^{197}Au mounted at the center of the scattering chamber. The ^{208}Pb target (thickness = 0.5 mg/cm^2) had a thin C (10 μg/cm^2) covering and a backing of 40 μg/cm^2 C. We assumed the ^{50}Ti^{12+} charge equilibrated in the 0.5 mg/cm^2 ^{208}Pb target and the equilibrium charge values [18] were used in calculating beam doses. The ^{197}Au target was 0.235 mg/cm^2 thick. The beam intensity was monitored by a shielded suppressed Faraday cup at the periphery of the

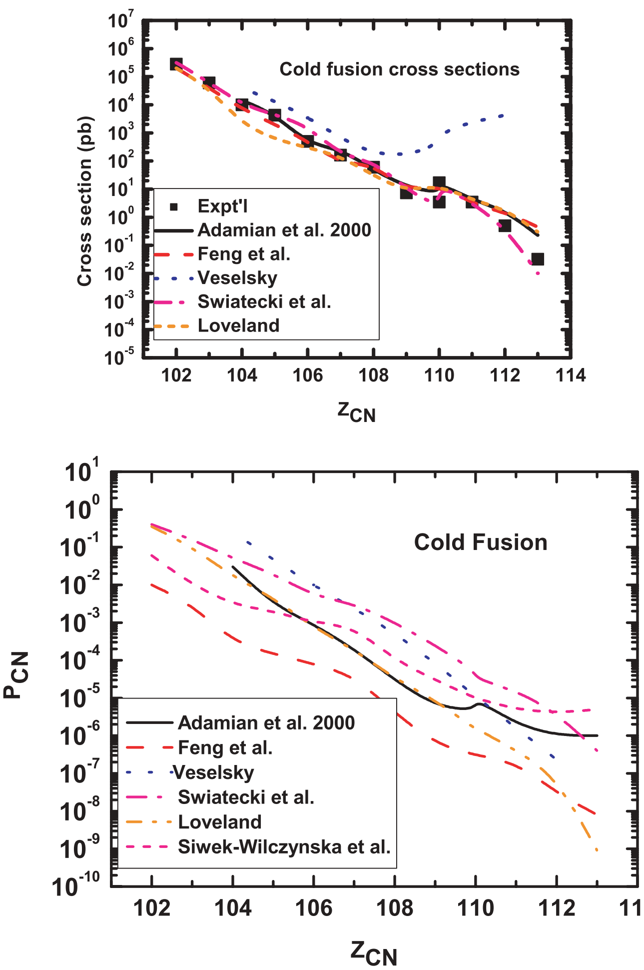

FIG. 1. (Color online) (a) Typical predictions of the formation cross sections of elements 102–113 using cold fusion reactions. (b) Comparison of predictions of P_{CN} for these cold fusion reactions.

chamber. A voltage of +10 kV was applied to the target to suppress the emission of energetic δ electrons, which, in a test run, had damaged the fission detectors. The beam intensities ranged from 1.1–4.9 $\times$ 10^{10} p/s. The beam energy loss in traversing half the target was calculated [19] and was typically 2.0 MeV.

At backward angles, an array of seven Si surface barrier detectors was mounted on a movable arm. The detector to target distance was 30 cm with each detector being 3 cm^2 in area with depletion depths ranging from 100 to 300 μm. Fission singles measurements were made for c.m. angles from 143 to 176° in small steps for each of the five projectile energies that were studied.

In addition to these individual Si detectors, two double sided strip detectors (DSSDs) were mounted on opposite sides of the beam. These Si strip detectors (Micron design W1) were 5 $\times$ 5 cm in area and were mounted at a distance of 22 cm from the target. Each detector consisted of 16 vertical strips on the front side and 16 horizontal strips on the back side. Due to a lack of readout electronics, the front strips were tied together in groups of two for readout and all 16 strips on the back side were tied together. Data from these strip detectors were recorded in the

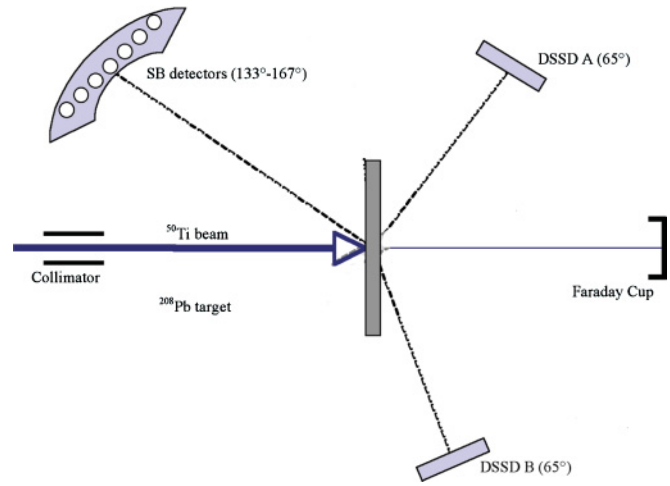

FIG. 2. (Color online) The schematic drawing of the experimental setup.

coincidence mode with the requirement (see below) that each detector was struck by a fission fragment (with rejection of deep inelastic and elastic events) and that the folding angle between the hits corresponded to a full momentum transfer event.

Time information was measured for each Si detector (surface barrier and strip) relative to the Linac pulse structure. The beam was bunched into packets with a FWHM of 0.65 ns. The average time between beam bursts was 82 ns. From the particle time of flight and energy, the mass of the fragment was calculated.

Energy calibrations of each Si detector were performed using the response of the detectors to radioactive decay α-particles (^{252}Cf) and elastically scattered beam from the ^{208}Pb and ^{197}Au targets. A correction for pulse height defect was applied to fission fragments striking the detectors, using the response of the detectors to ^{252}Cf fission fragments. [20]

The reaction of ^{50}Ti with ^{208}Pb can lead to elastic scattering, inelastic scattering, deep inelastic scattering, fusion-fission, quasifission, and fusion-evaporation residue formation. (The cross section for evaporation residue formation is small in comparison with the other processes and will be neglected in this discussion.) Fusion-fission and quasifission events were isolated from the other types of events by analyzing the E vs A response of each detector (Fig. 3). In Fig. 3, we show some typical singles data. Deep inelastic scattering of the ^{50}Ti projectile gives rise to the peak at $A \sim 50$. Fission fragments (from complete fusion-fission and quasifission) give rise to the broad bump in the center region of the plot. A gate was set on the fission events.

III. RESULTS

A. Capture cross sections

Two methods were used to deduce the capture-fission cross sections from the data. In the first method, the two strip detectors were used, operating in the coincidence mode. Each fission event was selected on the basis of having the correct

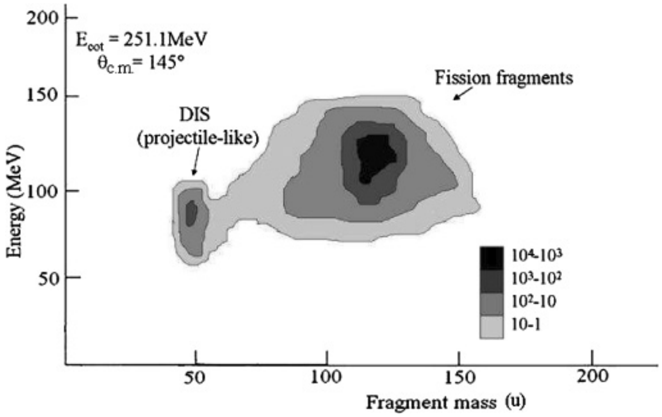

FIG. 3. Fragment energy vs mass for the reaction of 251 MeV ^{50}Ti with ^{208}Pb. The Si detector is positioned at $\theta_{c.m.}$ of 145°.

values of E and A and a folding angle corresponding to complete momentum transfer. Using one of the two detectors as a "trigger" detector, the geometric efficiency of the second detector was determined by simulations [21]. After correction for the efficiency of the second detector, a differential cross section, $d\sigma/d\Omega$ (θ) was calculated. The total cross section was deduced from this differential cross section by the simple assumption that the fission fragments were emitted in a plane perpendicular to the total angular momentum vector, i.e., the fragment angular distribution is given by

$$W(\theta) = (2\pi^2 \sin\theta)^{-1}. \tag{2}$$

Since the data are taken at angles near 90° in the c.m. system, the differences in corrections for missed events between this simple approximation and a more exact representation of the fragment angular distributions [23] should be less than 5%.

In the second method, the singles fission data at backward angles was integrated using data with $\theta_{lab} \leqslant 170°$ and fitting the data with Eq. (2). The results from this analysis were typically 10% less than the results from integrating the coincidence data. The two estimates of the capture-fission cross section were averaged to give the final values.

The resulting capture-fission cross sections are shown in Fig. 4 and Table I. In Fig. 4, we also show previous measurements [1,2] of $\sigma_{capture}$ for this reaction. The measured data from this work are in fair agreement with the measurements of Clerc *et al*. [2] and with the measurement of Bock *et al*. [1].

TABLE I. The measured capture-fission cross sections and the deduced values of P_{CN} and W_{sur} for ^{50}Ti+^{208}Pb. The c.m. beam energies are the energies calculated as corresponding to the center of the target beam energies. The errors are purely statistical.

$E_{c.m.}$ (MeV)	E^* (MeV)	$\sigma_{capture}$ (mb)	P_{CN}	W_{sur}
183.7	14.2	5.32 ± 0.57	0.020	2.6×10^{-5}
186.2	16.6	8.79 ± 0.91	0.049	7.1×10^{-6}
190.2	20.6	43.3 ± 1.9	0.27	2.4×10^{-7}
194.2	24.7	69.4 ± 0.9	0.33	5.1×10^{-8}
202.3	32.7	85.5 ± 7.3	0.19	1.0×10^{-8}

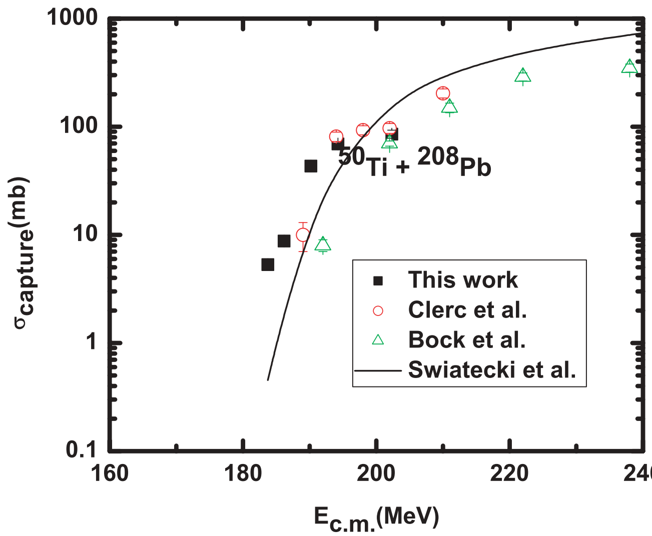

FIG. 4. (Color online) Capture-fission cross section for the reaction of ^{50}Ti with ^{208}Pb as measured in this work and [1,2]. The calculated cross section is from [5]. Two estimates of the one-dimensional barrier height for this reaction are 193.3 MeV [5] and 194.2 MeV [22].

Also shown in Fig. 4, are the predicted values of a widely-used semi-empirical model [5] for the capture cross sections for the ^{50}Ti+^{208}Pb reaction. The predicted values of $\sigma_{capture}$ increase more rapidly with increasing energy than any of the measured values.

B. Fragment angular distributions

The fission fragment angular distributions were measured using the individual Si detectors and are shown in Fig. 5.

It has been shown [11,25] that for reactions like the one studied in this work such as the ^{32}S+^{182}W and ^{32}S+^{208}Pb reactions that a significant fraction of the fission events result from "quasifission" as well as "true complete fusion". Quasifission is the process where the interacting nuclei merge to form a mononucleus but the system does not evolve inside the fission saddle point. For the purpose of estimating heavy element production by complete fusion, one must separate the contributions of quasifission and true complete fusion in the data. Using the methods outlined in Refs. [11,25] which depend on analyzing the shape of the fission fragment angular distributions, we have attempted to estimate the relative contributions of quasifission and complete fusion to the observed cross sections. The authors of [11,25] studied the angular distributions for a large number of reactions including some that were similar to the ones studied in this work (^{32}S+^{182}W, ^{208}Pb). They concluded that one could decompose the observed fission angular distributions into two components, one due to complete fusion and the other due to quasifission. The complete fusion component has an angular distribution characterized by values of the effective moment of inertia, $\Im_{eff}$, given by

$$\frac{\Im_0}{\Im_{eff}} = \max\,(c + dJ^2, 0.3) J \leqslant J_{cn} \tag{3}$$

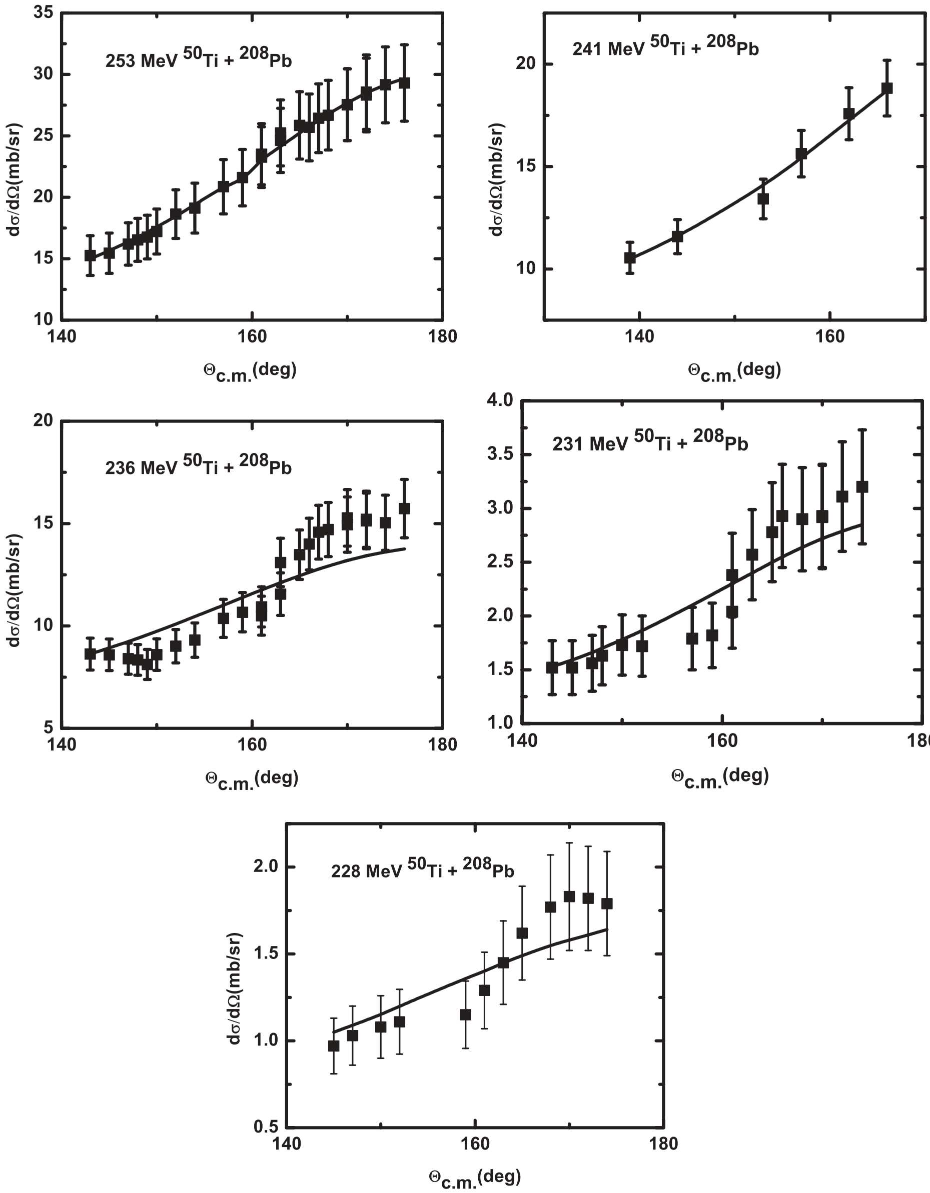

FIG. 5. Fission fragment angular distributions for the reaction of ^{50}Ti with ^{208}Pb. The measured data are shown along with fits to the data to determine the fraction of these events due to quasifission and the fraction due to complete fusion-fission.

while the quasifission component has

$$\frac{\Im_0}{\Im_{\rm eff}} = 1.5 J \succ J_{\rm cn}. \tag{4}$$

Figure 12 in [24] shows the shapes associated with various values of $\Im_0/\Im_{\rm eff}$ while the detailed logic behind equations [3] and [4] is discussed in Ref. [11]. Both the rotating liquid drop model and experimental data on complete fusion-fission reactions show that $\frac{\Im_0}{\Im_{\rm eff}}$ decreases linearly as the squared spin of the fissioning nucleus. The minimum value of $\frac{\Im_0}{\Im_{\rm eff}} = 0.3$ is chosen to simulate possible K breaking [11]. The choice of $\frac{\Im_0}{\Im_{\rm eff}} = 1.5$ for quasifission is arbitrary (see below).

In these equations, $\Im_0$ is the moment of inertia of a spherical nucleus with the same A value, complete fusion is assumed to occur for spins $0 \leqslant J \leqslant J_{\rm cn}$ and quasifission is assumed to occur for spins $J > J_{\rm cn}$. The constants c and d were shown to depend only on the fissility of the fissioning nucleus, x′, such that

$$x' = x_{\rm RLDM} + 0.3, \tag{5}$$

where the rotating liquid drop fissility, $x_{\rm RLDM}$ is given as

$$x_{\rm RLDM} = \frac{Z^2/{\rm A}}{50.883[1 - 1.7826[(N-Z)/A]^2]}. \tag{6}$$

Values of $c = 0.75$ and $d = -0.000135$ were used in the calculations [11]. We fitted the observed fission fragment angular distributions for center of mass projectile energies of 184–202 MeV, allowing the maximum angular momentum associated with complete fusion, $J_{\rm CN}$, to be a free parameter determined in the calculation. ($J_{\rm max}$ was determined by the total fission cross section using a sharp cutoff approximation.) We used the familiar expressions for the fission fragment angular distributions [23]:

$$W(\theta) = \sum_{J=0}^{J_{CN}} \frac{(2J+1)^2 \exp\left[-(J+1/2)^2 \sin^2\theta / 4K_0^2(FF)\right] J_0\left[i(J+1/2)^2 \sin^2\theta / 4K_0^2(FF)\right]}{erf\left[(J+1/2)/\left(2K_0^2(FF)\right)^{1/2}\right]} + \sum_{J=J_{CN}}^{J_{max}} \frac{(2J+1)^2 \exp\left[-(J+1/2)^2 \sin^2\theta / 4K_0^2(QF)\right] J_0\left[i(J+1/2)^2 \sin^2\theta / 4K_0^2(QF)\right]}{erf\left[(J+1/2)/\left(2K_0^2(QF)\right)^{1/2}\right]} \quad (7)$$

assuming $M = 0$, i.e., assuming the spins of the target and projectile were zero, where J_0 is the zero order Bessel function with imaginary argument and the error function $erf[(J+1/2)/(2K_0^2)^{1/2}]$ is defined as

$$erf(x) = (2/\pi^{1/2}) \int_0^x \exp(-t^2) dt. \quad (8)$$

The parameter K_0^2 is defined as

$$K_0^2 = T\Im_{\mathrm{eff}}/\hbar^2, \quad (9)$$

$$\frac{1}{\Im_{\mathrm{eff}}} = \frac{1}{\Im_{\parallel}} - \frac{1}{\Im_{\perp}}, \quad (10)$$

where the nuclear temperature at the saddle point T is given as

$$T = \left[\frac{E^* - B_f - E_{\mathrm{rot}}}{A/8.5}\right]^{1/2} \quad (11)$$

and $\Im_{\parallel}$ and $\Im_{\perp}$ are the moments of inertia for rotations around the axis parallel and perpendicular to the nuclear symmetry axis, respectively. B_f and E_{rot} are the fission barrier and rotational energy of the system. The assumption that

$$\frac{\Im_0}{\Im_{\mathrm{eff}}} = 1.5 \quad \text{for} \quad J \succ J_{cn}$$

for quasifission is arbitrary. The value of this ratio is greater than that observed in any complete fusion-fission reaction for this fissility [11] but the actual value of this ratio is not well established. Recently Nasirov *et al.* [26] have calculated the moments of inertia of the quasifissioning system using the dinuclear system (DNS) approach. For the similar $^{32}S + ^{208}Pb$ reaction, their calculated values of $\frac{\Im_0}{\Im_{\mathrm{eff}}}$ range from 1.7 to 2.9 depending on the energy of the incident projectile. We have chosen to analyze our angular distribution data in two ways: (a) assume $\frac{\Im_0}{\Im_{\mathrm{eff}}} = 1.5$, the "classical Back analysis" and (b) assume values of $\frac{\Im_0}{\Im_{\mathrm{eff}}}$ similar to those predicted for the $^{32}S+^{208}Pb$ reaction by Nasirov *et al.* [26].

In fitting the angular distribution data, one uses the measured value of $\sigma_{\mathrm{capture}}$, uses a sharp cutoff J_{capture} value deduced from

$$J_{\mathrm{capture}} = \left(\frac{\sigma_{\mathrm{capture}}}{\pi \lambda\!\!\!^{-2}}\right)^{1/2} - 1 \quad (12)$$

and K_0^2 values calculated from Eqs. (5) and (6) and varies J_{CN} in Eq. (3) until a minimum in the reduced chi-square, χ_ν^2, is achieved. Then

$$\frac{J_{CN}^2}{J_{max}^2} = \frac{\sigma_{CN}}{\sigma_{\mathrm{capture}}} = P_{CN}. \quad (13)$$

For excitation energies of 14.2, 16.6, 20.6, 24.7, and 32.7 MeV, the deduced values of P_{CN} for method (b) were 0.02, 0.049, 0.27, 0.33, and 0.19, respectively. Using method (a) above, the deduced P_{CN} values were 0.02, 0.049, 0.23, 0.18, and 0.22. For all cases, the χ_ν^2 values were statistically significant at the 95% level [28]. We show, in Fig. 5, the fits to the data using method (b), which we prefer, as being a less arbitrary way to specify $\frac{\Im_0}{\Im_{\mathrm{eff}}}$. The deduced values of P_{CN} are shown in Fig. 6 along with various predictions of this quantity. In Fig. 6, we also show the result of an investigation of the $^{50}Ti+^{208}Pb$ reaction by Itkis *et al.* [27] in which a value of P_{CN} was deduced from an analysis of the widths of the fission mass distributions. It is encouraging to note that the two methods of deducing P_{CN} give similar results for this system.

It is difficult to make meaningful estimates of the uncertainties in the deduced values of P_{CN} given the fundamental systematic uncertainties in $\frac{\Im_0}{\Im_{\mathrm{eff}}}$ and thus in K_0^2. One estimate of the uncertainty in the deduced values of P_{CN} is from the comparison between the deduced values of P_{CN} based upon the fragment angular distributions (this work) and the fragment mass distributions [27] which correspond to an uncertainty of

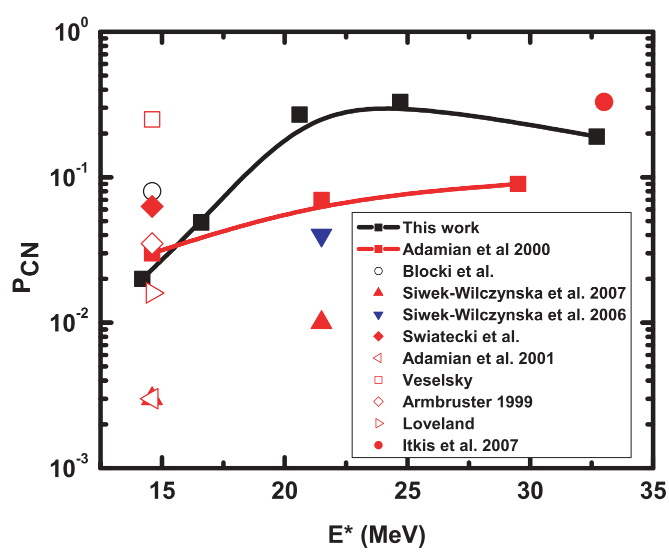

FIG. 6. (Color online) Deduced values of P_{CN} from this work for the $^{50}Ti+^{208}Pb$ reaction compared to various estimates of this quantity [7,30,10,33,5,31,9,29,6] and the measurements of Itkis *et al.* [27]. The maxima of the $1n$, $2n$, and $3n$ excitation functions are at ~15, 22, and 30 MeV, respectively [15].

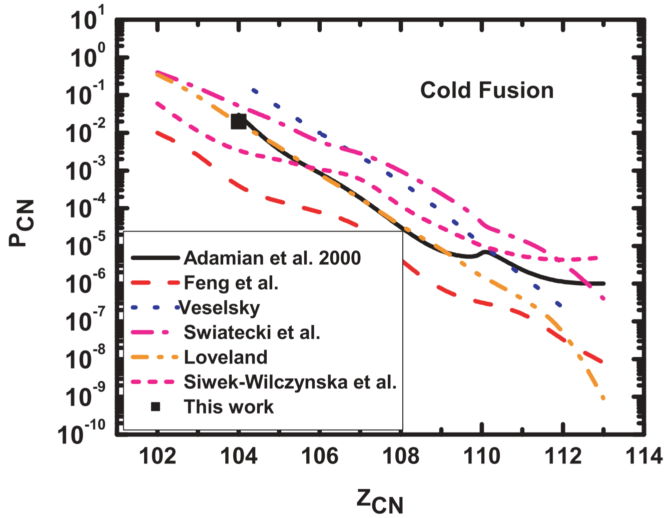

FIG. 7. (Color online) Comparison of the value of P_{CN} deduced in this work with the data of Fig. 1(b).

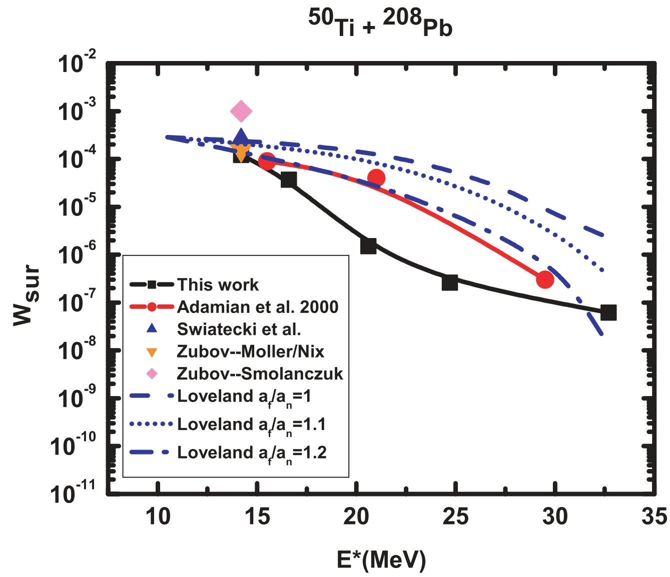

FIG. 8. (Color online) Deduced values of W_{sur} from this work for the ^{50}Ti +^{208}Pb reaction compared to various estimates of this quantity [7,5,34,6].

a factor of 1.8. The uncertainties in the deduced values of P_{CN} due to differing assumptions about K_0^2 amount to an average factor of 1.2.

Straightforwardly, we can write

$$W_{sur} = \frac{\sigma_{EVR}}{\sigma_{CN}} \tag{14}$$

and we have used this equation to calculate W_{sur} (Fig. 7). There is a systematic uncertainty in these deduced W_{sur} values due to uncertainties in the measured values of σ_{EVR} for the ^{50}Ti+^{208}Pb system. For example, at the maximum of the ^{208}Pb(^{50}Ti, n) excitation function, Hessberger *et al.* [14] measured σ_{EVR} to be 10±1 nb, Hofmann *et al.* [15] report $\sigma_{EVR} = 16$ nb while preliminary results from a recent measurement of Dragojevic and Gregorich [16] indicate $\sigma_{EVR} = 43^{+9.9}_{-8.2}$nb. These differences in measured values of σ_{EVR} may be more apparent than real (due to differing values of the widths of the excitation energy bins). We have chosen to use the data of Hofmann *et al.* [15] as representing the most complete data set that spans the range of excitation energies used in this work. Nonetheless, it is possible that if there is a systematic error in σ_{EVR}, our estimates of W_{sur} could be a factor of 2.7 too low.

IV. DISCUSSION

In Fig. 6, we compare the deduced values of P_{CN} for the ^{50}Ti +^{208}Pb reaction with various calculations of this quantity. Most of the calculations are for an excitation energy of ~15 MeV, i.e., the peak of the 1n excitation function. One group of predictions [6,7,29] are very close to the deduced value of P_{CN} for the 1n reaction. Of these estimates, two [6,29] are semiempirical fits to data while the third [7] is a DNS model calculation of P_{CN}. Two calculations [5,30] based on the "fusion by diffusion" model are within a factor of 4 of the deduced value, while there are a set of outlyers that differ from the deduced value by an order of magnitude [9,10,31]. The deduced change in P_{CN} in going from the maximum of the 1n excitation function to the maximum of the 2n excitation function is much greater than most models expect [7,10,33]. It should be noted that Zagrebaev *et al.* [32] have suggested that

$$P_{CN}(E^*) = \frac{P_0}{1 + \exp\left(\frac{(E_0 - E^*)}{\Delta}\right)}, \tag{15}$$

where E_0 and Δ are empirical constants and $P_0 = 1$. Taking $E_0 = 30$ MeV and $\Delta = 2$ MeV [32] allows one to roughly estimate the increase in P_{CN} in going from $E^* = 14.2$ MeV to $E^* = 20.6$ MeV to be ~24, which is similar to the deduced value of ~14. To put this measurement in perspective, we show, in Fig. 7, the value of P_{CN} deduced for the ^{208}Pb(^{50}Ti,n) reaction compared with the data of Fig. 1(b).

The situation with regard to survival probabilities (Fig. 8) for the single chance fission 1n reaction seems better. Apart from the calculation by Zubov *et al.* [34] using masses due to Smolanczuk [35], there is fair agreement between the deduced and predicted values of W_{sur}, especially considering the possibility of a systematic underestimate (of a factor of 2.7) of W_{sur} in this work due to uncertainties in σ_{EVR}. Of greater concern are the deviations between the predicted and deduced values of the survival probabilities for the multiple chance fission reactions, which are intrinsically harder to predict. To better understand the nature of this discrepancy, we refer to the simple model of the survival probabilities used by Loveland [6]. In this formalism, the survival probability W_{sur} can be written as

$$W_{sur} = P_{xn}(E^*) \prod_{i=1}^{i_{max}=x} \left(\frac{\Gamma_n}{\Gamma_n + \Gamma_f}\right)_{i,E^*}, \tag{16}$$

where the index i is equal to the number of emitted neutrons and P_{xn} is the probability of emitting exactly x neutrons [36]. In evaluating the excitation energy, one starts at the excitation energy E^* of the completely fused system and reduces it for each evaporation step by the binding energy of the emitted neutron and an assumed neutron kinetic energy of $2T$ where

$T(=(E^*/a)^{1/2})$ is the temperature of the emitting system. For calculating Γ_n/Γ_f, one uses the classical formalism from Vandenbosch and Huizenga [37]

$$\frac{\Gamma_n}{\Gamma_f} = \frac{4A^{2/3}a_f(E^* - B_n)}{ka_n\left[2a_f^{1/2}(E^* - B_f)^{1/2} - 1\right]} \exp\left[2a_n^{1/2}(E^* - B_n)^{1/2} - 2a_f^{1/2}(E^* - B_f)^{1/2}\right], \quad (17)$$

where a_f and a_n are the level density parameters at the saddle point and the equilibrium deformation. The constant k is taken to be 9.8 MeV and $a_n = A/12$. The fission barriers, B_f, are written as the sum of liquid drop, B_f^{LD}, and shell correction terms as

$$B_f(E^*_{\rm CN}) = B_f^{LD} + U_{\rm shell}\exp[-\gamma E^*], \quad (18)$$

where

$$\gamma^{-1} = 5.48A^{1/3}/\left(1 + 1.3A^{-1/3}\right)\text{MeV}, \quad (19)$$

where the shell correction energies, $U_{\rm shell}$, to the LDM barriers are taken from [38], the liquid drop barriers are taken from [39] and the fade-out of the shell corrections with increasing excitation energy are taken from Ignatyuk *et al*. [40]. Neutron binding energies, B_n, are taken from [38]. Collective enhancement effects are only important for spherical product nuclei and they are calculated using the semiempirical formalism of [41] where the collective enhancement factor multiplies $\frac{\Gamma_n}{\Gamma_f}$ and is written as $K_{\rm vib}/K_{\rm rot}f(E^*/E_{\rm crit})$ where $K_{\rm rot} = 1.4 \times 10^{-2}A^{5/3}T(1 + \beta_2/3)$ where β_2 is the deformation parameter and $K_{\rm vib} = (1 + 0.14\Delta N + 0.23\Delta Z)^2$ where ΔN and ΔZ are the numbers of valence nucleons or valence holes with respect to the next doubly closed shell nucleus with $f(E^*/E_{\rm crit}) = [1 + \exp((E^* - E_{\rm crit})/d_{\rm crit})]^{-1}$ where $E_{\rm crit} = 40$ MeV and $d_{\rm crit} = 10$ MeV. This simple formalism should have the virtue of allowing one to understand the physical factors that affect the survival probabilities.

In this formalism, the energy dependence of the survival probabilities is contained in the Vandenbosch-Huizenga general formula and the energy dependence of the shell correction. Since this formalism correctly predicts the survival probability for the $1n$ reaction, one would expect, with an appropriate way to treat the effect of excitation energy, a correct prediction of the survival probabilities at higher energies. In Fig. 8, we show some calculations of the survival probabilities as a function of the excitation energy E^*, assuming various values of the ratio of the level density parameters, a_f/a_n. The data seem to suggest that a_f/a_n is greater than unity. Possible explanations for this behavior are discussed in [37]. The point is that reasonable assumptions about the level density at the saddle point and the equilibrium deformation are roughly consistent with the observed behavior of the survival probabilities although a detailed description of these survival probabilities is not yet available.

The deduced data on $P_{\rm CN}$ and $W_{\rm sur}$ from this work should serve to further challenge and guide our attempts to understand the synthesis of heavy nuclei using cold fusion reactions. It is clear that the data on $P_{\rm CN}$ and its excitation energy dependence is best described in terms of the dinuclear systems (DNS) approach to describing these reactions. From an experimental point of view, detailed studies of the excitation energy dependence of the survival probabilities for very heavy systems would seem valuable, especially those involving direct physical measurements of the emitted neutrons. From the point of view of nuclear theory, it should be possible to calculate the nuclear level density for the equilibrium and saddle point deformations using our current knowledge of what we believe the single particle levels are in these nuclei and their shifts with deformation. Such calculations would seem to be an essential part of our understanding of the properties of the heaviest nuclei.

V. CONCLUSION

What have we learned in this study? We have (a) made some of the first experimental deductions of $P_{\rm CN}$ for a cold fusion reaction at the maximum of the $1n$ excitation function as well as deducing the survival probabilities at this excitation energy (b) compared these deduced quantities with theoretical estimates of these quantities showing the semiempirical estimates and DNS model calculations do the best job of reproducing the data and (c) found that several models have trouble correctly predicting the energy dependence of $P_{\rm CN}$ and $W_{\rm sur}$.

ACKNOWLEDGMENTS

We thank John Greene for preparing the ^{208}Pb targets used in this experiment. We gratefully acknowledge helpful discussions with K.E. Gregorich and thank him for his careful reading of this manuscript. This work was supported in part by the Director, Office of Energy Research, Division of Nuclear Physics of the Office of High Energy and Nuclear Physics of the U.S. Department of Energy under Grant Nos. DE-FG06-97ER41026 and DE-FG06-94ER40848.

[1] R. Bock *et al*., Nucl. Phys. **A388**, 334 (1982).
[2] H.-G. Clerc, J. G. Keller, C.-C. Sahm, K.-H. Schmidt, H. Schulte, and D. Vermeulen, Nucl. Phys. **A419**, 571 (1984).
[3] A. J. Pacheco *et al*., Phys. Rev. C **45**, 2861 (1992).
[4] E. V. Prokhorova *et al*., *Exotic Nuclei, International Symposium* (World Scientific, Singapore, 2004), pp. 325–332.
[5] W. J. Swiatecki, K. Siwek-Wilczynska, and J. Wilczynski, Phys. Rev. C **71**, 014602 (2005).
[6] W. Loveland, Phys. Rev. C **76**, 014612 (2007).
[7] G. G. Adamian, N. V. Antonenko, and W. Scheid, Nucl. Phys. **A678**, 24 (2000).
[8] Z.-Q. Feng, G.-M. Jin, J.-Q. Li, and W. Scheid, Phys. Rev. C **76**, 044606 (2007).
[9] M. Veselsky, Acta Phys. Slovaca **49**, 101 (1999).
[10] K. Siwek-Wilczynska, I. Skwira-Chalot, and J. Wilczynski, Int. J. Mod. Phys. E **16**, 483 (2007).
[11] B. B. Back, Phys. Rev. C **31**, 2104 (1985).
[12] F. P. Hessberger *et al*., Z. Phys. A **321**, 317 (1985).

[13] F. P. Hessberger *et al.*, Z. Phys. A **359**, 415 (1997).
[14] F. P. Hessberger *et al.*, Eur. Phys. J. A **12**, 52 (2001).
[15] S. Hofmann *et al.*, Nucl. Phys. **A734**, 93 (2004).
[16] K. E. Gregorich and I. Dragojevic (private communication), 2007.
[17] Y. T. Oganessian *et al.*, Z. Phys. A **319**, 215 (1984).
[18] K. Shima, T. Ishihara, and T. Mizumo, Nucl. Instrum. Methods **200**, 605 (1982).
[19] J. F. Ziegler, Nucl. Instrum. Methods Phys. Res. B **219**, 1027 (2004).
[20] H. W. Schmitt, W. E. Kiker, and C. W. Williams, Phys. Rev. **137**, B837 (1965).
[21] E. Duek, L. Kowalski, and J. M. Alexander, Comput. Phys. Commun. **34**, 395 (1985).
[22] R. Bass, Phys. Rev. Lett. **39**, 265 (1977).
[23] J. R. Huizenga, A. N. Behkami, and L. G. Moretto, Phys. Rev. **177**, 1826 (1969).
[24] M. B. Tsang *et al.*, Phys. Rev. C **28**, 747 (1983).
[25] J. G. Keller *et al.*, Phys. Rev. C **36**, 1364 (1987).
[26] A. K. Nasirov, R. K. Utamuratov, G. Fazio, G. Giardina, F. Hanappe, G. Mandaglio, M. Manganoro, and W. Scheid, Eur. Phys. J. A (submitted); see arXiv:0705.2748v1.
[27] M. G. Itkis *et al.*, Nucl. Phys. **A787**, 150c (2007).
[28] L. Lyons, *A Practical Guide to Data Analysis for Physical Science Students* (Cambridge University Press, Cambridge, 1991).
[29] P. Armbruster, Rep. Prog. Phys. **62**, 465 (1999).
[30] J. Blocki, L. Shvedov, and J. Wilczynski, Int. J. Mod. Phys. E **15**, 426 (2006).
[31] G. G. Adamian, N. V. Antonenko, A. Diaz-Torres, S. P. Ivanova, W. Scheid, and V. V. Volkov, Acta Phys. Hungarica, Heavy Ion Phys. **14**, 3 (2001).
[32] V. I. Zagrebaev, Y. Aritomo, M. G. Itkis, Y. T. Oganessian, and M. Ohta, Phys. Rev. C **65**, 014607 (2001).
[33] K. Siwek-Wilczynska, I. Skwira-Chalot, and J. Wilczynski, AIP Conf. Proc. **853**, 265 (2006).
[34] A. S. Zubov, G. G. Adamian, N. V. Antonenko, S. P. Ivanova, and W. Scheid, Phys. Rev. C **65**, 024308 (2002).
[35] R. Smolanczuk, J. Skalski, and A. Sobiczewski, Phys. Rev. C **52**, 1871 (1995); R. Smolanczuk, *ibid.* **59**, 2634 (1999).
[36] J. D. Jackson, Can. J. Phys. **34**, 767 (1956).
[37] R. Vandenbosch and J. R. Huizenga, *Nuclear Fission* (Academic, New York, 1973), p. 323.
[38] P. Moller, J. R. Nix, W. D. Myers, and W. J. Swiatecki, At. Data Nucl. Data Tables **59**, 185 (1995).
[39] W. D. Myers and W. J. Swiatecki, Phys. Rev. C **60**, 014606 (1999).
[40] A. Ignatyuk *et al.*, Sov. J. Nucl. Phys. **21**, 612 (1975).
[41] P. Armbruster, Annu. Rev. Nucl. Part. Sci. **50**, 411 (2000).